Seismic Acoustic Ratio Estimates Using a Moving Vehicle Source

Roy Greenfield*, Mark Moran[+]

August 1999

* Dept. Geosciences, Penn State University
504 Deike Building
University Park, PA 16802
814-865-5723
roy@geosc.psu.edu

+ USA CRREL
72 Lyme Rd, Hanover NH 03755-1290
603-646-4274
mmoran@crrel.usace.army.mil

ABSTRACT

Seismic and acoustic noise from moving tracked vehicles was used to determine the seismic to acoustic signal coupling ratio (SAR) in the ground. The seismic signal received on a geophone contains some energy that has propagated as seismic waves and some energy that couples from acoustic waves to seismic waves in the vicinity of the geophone. We use the frequency domain coherence between the microphone and geophone signals to determine when the seismic signal is predominantly due to acoustic to seismic wave coupling. In frequency bands where the microphone and geophone coherence is above 0.8 the ratio of the seismic ground particle velocity to sound pressure, SAR, can be determined with less than 2 dB of error. The method is applied to data from a summer experiment with grass ground cover and at two winter experiments with snow covered ground. At 100 Hz, the summer analysis yields a SAR of $1x10^{-5}$ [(m/s)/Pa]. Also at 100 Hz, the two winter analyses yield SAR values of 0.1 and $1.0x10^{-5}$ [(m/s)/Pa]. In the later result the SAR using blank pistol shots gives very close values. These results can be used to remove acoustic contamination from seismic signals. We also show a loose correlation between the SAR values and the shear strength of the ground

1.0 INTRODUCTION

It is well established that sound waves move the earth and create signals on a geophone. The coupling of sound to geophones has been studied using stationary sources such as speakers (e.g. Sabatier et al. 1986a, 1986b) and blank pistol shots (Albert and Orcutt, 1989). The measurement normally made is the ratio of the seismic ground motion velocity divided by sound pressure. We denote this quantity as SAR. This SAR has been used with other measurements to get properties of the ground (e.g., Sprague et al., 1993). It is also important to measure SAR if full use is to be made of seismic signals in area monitoring activities.

In this work we determine the SAR using signals generated by moving military vehicles. This is useful in situations where a controlled source cannot be used, or when the properties of the ground surface are changing, such as in snow-covered or freezing ground. In these circumstances the SAR will also change, and it is convenient to have methods that do not require a carefully controlled source. Energy from a moving vehicle produces a geophone signal in several ways. Vehicle treads mechanically vibrate the ground, causing seismic waves. Next acoustic energy from engine exhaust can vibrate the ground in the immediate vicinity of the vehicle, generating seismic waves that travel to geophone. And, finally,

REPORT DOCUMENTATION PAGE

1. REPORT DATE (DD-MM-YYYY) 01-08-1999	2. REPORT TYPE	3. DATES COVERED (FROM - TO) xx-xx-1999 to xx-xx-1999
4. TITLE AND SUBTITLE Seismic Acoustic Ratio Estimates Using a Moving Vehicle Source Unclassified	**5a. CONTRACT NUMBER**	
	5b. GRANT NUMBER	
	5c. PROGRAM ELEMENT NUMBER	
6. AUTHOR(S) Greenfield, Roy ; Moran, Mark ;	**5d. PROJECT NUMBER**	
	5e. TASK NUMBER	
	5f. WORK UNIT NUMBER	
7. PERFORMING ORGANIZATION NAME AND ADDRESS USA CRREL 72 Lyme Rd Hanover , NH 03755-1290	**8. PERFORMING ORGANIZATION REPORT NUMBER**	
9. SPONSORING/MONITORING AGENCY NAME AND ADDRESS ,	**10. SPONSOR/MONITOR'S ACRONYM(S)**	
	11. SPONSOR/MONITOR'S REPORT NUMBER(S)	
12. DISTRIBUTION/AVAILABILITY STATEMENT A PUBLIC RELEASE ,		

13. SUPPLEMENTARY NOTES

14. ABSTRACT
Seismic and acoustic noise from moving tracked vehicles was used to determine the seismic to acoustic signal coupling ratio (SAR) in the ground. The seismic signal received on a geophone contains some energy that has propagated as seismic waves and some energy that couples from acoustic waves to seismic waves in the vicinity of the geophone. We use the frequency domain coherence between the microphone and geophone signals to determine when the seismic signal is predominantly due to acoustic to seismic wave coupling. In frequency bands where the microphone and geophone coherence is above 0.8 the ratio of the seismic ground particle velocity to sound pressure, SAR, can be determined with less than 2 dB of error. The method is applied to data from a summer experiment with grass ground cover and at two winter experiments with snow covered ground. At 100 Hz, the summer analysis yields a SAR of 1x10 -5 [(m/s)/Pa]. Also at 100 Hz, the two winter analyses yield SAR values of 0.1 and 1.0x10 -5 [(m/s)/Pa]. In the later result the SAR using blank pistol shots gives very close values. These results can be used to remove acoustic contamination from seismic signals. We also show a loose correlation between the SAR values and the shear strength of the ground

15. SUBJECT TERMS

16. SECURITY CLASSIFICATION OF:			17. LIMITATION OF ABSTRACT	18. NUMBER OF PAGES	19a. NAME OF RESPONSIBLE PERSON
			Public Release	12	Fenster, Lynn lfenster@dtic.mil
a. REPORT Unclassified	**b. ABSTRACT** Unclassified	**c. THIS PAGE** Unclassified			**19b. TELEPHONE NUMBER International Area Code** **Area Code Telephone Number** 703 767-9007 **DSN** 427-9007

energy propagates as sound waves and vibrates the ground near the geophone. The variety of propagation paths and signal excitation mechanisms from a moving vehicle, rather than a speaker or pistol source, requires extra care in data reduction.

To estimate the SAR, we must determine which part of the total seismic signal has propagated as sound waves. To do this we look at the coincidence of power spectral density peaks from microphone and geophone signals, and at the spectral coherence between microphone and geophone signals. We apply our method of SAR determination to three sites and compare the results to previously reported findings.

2.0 METHODS

2.1 Site Descriptions

Data will be discussed from three field experiments. The first data set, denoted as Aberdeen, was taken at Aberdeen Proving Ground, MD. Data were taken in a large open field, with grass cover, throughout the evening and into the early morning hours of 28 October 1998. Topographic relief between the vehicle source and the sensor locations is less than 1 m. The area geology a is low elevation island with thick overburden soils and tidal marsh. At the recording site, the depth to the water table is roughly 1 m. Air temperature at 1 m above ground level was approximately 20°C in the early evening and dropped to 0°C in the early morning. The average wind speeds over the course of the recording period were less than 1 m/s. A small shallow hole, roughly the height of the geophone, was stamped through the grass and the spiked geophones were pushed into the compacted earth. The microphone and vertical geophone were separated by approximately 9 m. An example of the data from this site are shown in Figure 1. Data from several sections of this record were analyzed.

The second data set, called Alaska I, uses data collected at the Texas Range, Cold Regions Test Center (CRTC), Ft. Greely, Alaska. The data were taken 27 January 1998 during a day with low wind (2 km/hr), and air temperatures below $–17^{o}$C. The site was located adjacent to low-lying hills associated with Donnely Dome glacial deposits (Pewe, 1964). The area is characterized by deep glacial tills and extensive permafrost (Arcone et al., 1998). The ground was frozen to a depth of at least 1 m and an extensive snow cover varied in depth between 15 and 60 cm. The average snow density was 0.6 g/cm^3. The area is largely open with only short (<1 m) scrubby vegetation. Vehicles traveled along a dirt road. No topography of vegetation obscured line of sight between the sensors and vehicles. Geophones mounted on spikes were forced into predrilled holes in the ground. The microphones were mounded on stands 1 m above the snow surface. The data analyzed are from a microphone separated by 3 m from a vertical geophone.

A third data set, called Alaska II, was collected on 11 December 1997 at the Texas Range, CRTC, Ft. Greely, Alaska. The average midday air temperature was $–15^{o}$C and wind speed was less than 5 km/hr. The collection site was approximately 2000 m to the northwest of the Alaska I data collection area and well outside the Donnely Dome glacial deposits. This region is dominated by fluvial glacial outwash deposited by the Delta River, a braided river system draining the Black Rapids Glacier (Pewe, 1964). The river was 2000 m further to the northwest of the Alaska II site. The immediate vicinity of this site was bordered to the east with open low lying vegetation (< 1 m high). A hundred meters the west were dense groves of 2-to-3-m-high willows. The maximum topographic variation within the recording region was less than 1 m. The sensors were placed 25 m to the west of a dirt road, which was oriented roughly north-south. No topography or vegetation obscured the line-of-sight between the vehicles on road and the sensor positions. Microphones were placed on stands 30 cm above a dense crusty snow layer that was roughly 10 cm thick and intermittent in areal extent. The average snow density was 0.4 g/cm^3. Similarly to the Alaska I data, the Alaska II data were produced by geophones driven into undersized holes drilled in the frozen soil. The offset between the microphone and vertical geophone was approximately 30 cm.
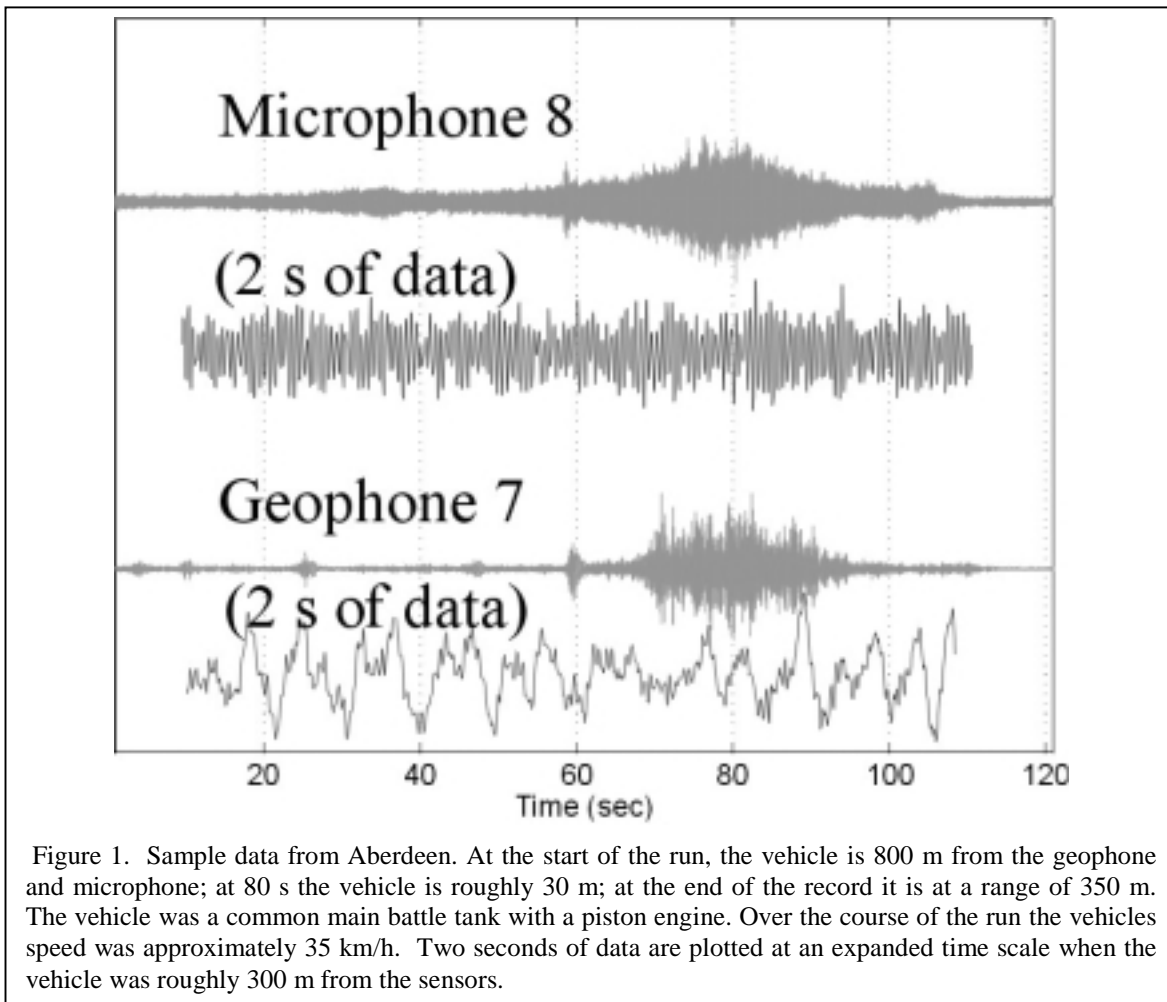
Figure 1. Sample data from Aberdeen. At the start of the run, the vehicle is 800 m from the geophone and microphone; at 80 s the vehicle is roughly 30 m; at the end of the record it is at a range of 350 m. The vehicle was a common main battle tank with a piston engine. Over the course of the run the vehicles speed was approximately 35 km/h. Two seconds of data are plotted at an expanded time scale when the vehicle was roughly 300 m from the sensors.

2.2 Data Recording

All seismic and acoustic signals were recorded simultaneously on a 16-bit, digital seismograph. The seismograph uses an analogue 3-Hz high pass filter and a digital anti-alias low pass filter that is appropriate for the time sample selected for the recordings. Sampling rates were 500 samples/s for Aberdeen, and 1000 samples/s for both Alaska sets. Fixed system gains are placed in the digital recording. The seismograph automatically places scaling values in the header of each recording, allowing conversion of the recorded data from digital counts to the input voltage. In off-line processing, the system gain is considered in the conversion from digital counts to physical units. Mark Products 4.5-Hz (resonant frequency) geophones were used to sense ground motion. The geophone response is flat in velocity ($<$ 3 dB variation) between 4 and 500 Hz when operating in a temperature range between -40°C and 65°C. Bruel & Kjaer 4165 all-weather, capacitance, free-field, broadband microphones with windscreens were used for the acoustic measurements. The microphone transducer response is flat ($<$3 dB variation) between 3 and 200 kHz. The operation temperature range for these transducers is between -30°C and 100°C. Custom preamplifier units interface the microphones directly to the seismograph. Laboratory bench measurements showed no preamplifier amplitude or phase distortions between 5 and 50 kHz.

The recording scale factors depend on the largest amplitudes of all the recorded signals and the system gain setting. To convert the seismic signals to physical units we used the published conversion parameter for the 4.5-Hz Mark Products geophone of 32.2 V/(m/s). Microphone sound pressure level (SPL) calibration was done in the field using a General Radio SPL calibrator that used a 125-Hz source with an amplitude of 114 dB relative to 20 μPa.

2.3 Calculation Methods

The seismic signal recorded on a geophone is made up of several components: 1) Energy that propagates from the vehicle source to the receiver as seismic surface or body waves, 2) energy that propagates as sound in the air and couples to the earth near the geophone, and 3) energy that is from sources other than the vehicle. This is depicted in Figure 2. The sound will move the ground near the geophone to creating a signal on the geophone. This part of the geophone signal will be coherent with the sound on a microphone positioned near the geophone. Energy that comes to the geophone as a seismic wave will not be coherent with the microphone signal. Thus part of the geophone signal will be coherent with the microphone signal, as shown in Figure 3. As shown, both instruments will have coherent and incoherent signal components.
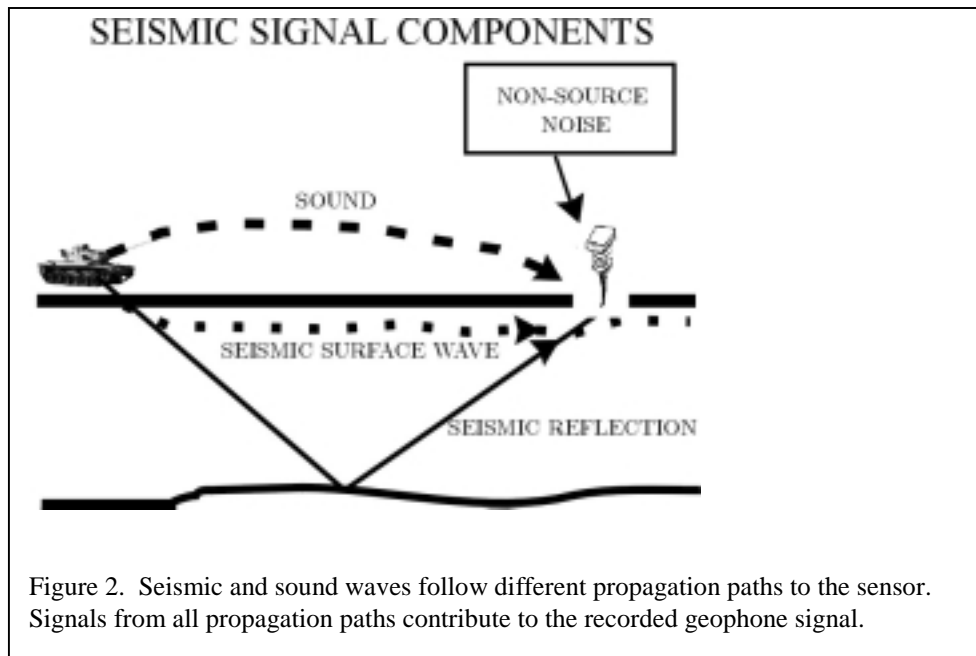

Figure 2. Seismic and sound waves follow different propagation paths to the sensor. Signals from all propagation paths contribute to the recorded geophone signal.
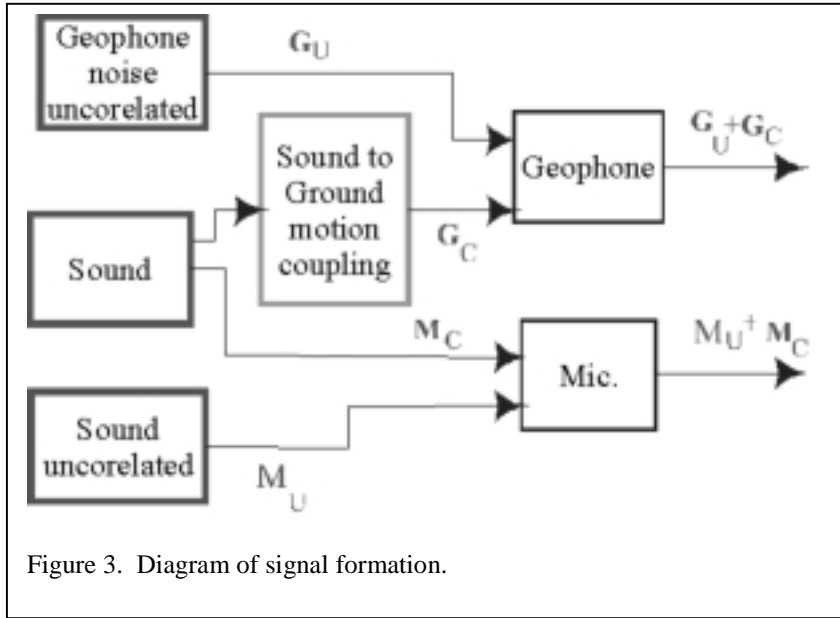
Figure 3. Diagram of signal formation.

The coherence is a measure of the similarity of the seismic and acoustic signal. Relative to a microphone signal, the geophone signal is composed of uncorrelated energy (Gu) that propagates through the earth and correlated energy (Gc) that has propagated to the vicinity of the geophone as sound. Relative to the geophone signal, the microphone signal is composed of correlated vehicle energy (that couples into the ground), Mc, and other uncorrelated sound, Mu, for example wind noise. The total microphone signal is then the correlated and the uncorrelated parts, $Mc + Mu$, while the total geophone signal is $Gc + Gu$. The frequency domain coherence is defined as

$$C \equiv \frac{\left| \left(P_{MG} \right) \right|^2}{\left(P_{MM} \right)\left(P_{GG} \right)} = \left| \frac{\left(P_{Mc} P_{Gc} \right)}{\left(P_{Mu} + P_{Mc} \right)\left(P_{Gu} + P_{Gc} \right)} \right| \qquad (1)$$

where

$P_{MM}, P_{GG} \equiv$ microphone and geophone power spectra

$P_{MG} \equiv$ microphone and geophone cross power spectra

P_{Mu} and P_{Mc} are the microphone incoherent and coherent parts

P_{Gu} and P_{Gc} are the geophone incoherent and coherent parts.

Estimating the coherence using a block averaging method gives a measure of how constant the phase difference between microphone and geophone signals are between blocks. Thus the coherence is a measure of how much of the energy is common to both traces, as given by equation (1). If C is close to 1, C is given to first order (in uncorrelated power over correlated power) by

$$C \cong 1 - \left(\frac{P_{Gu}}{P_{GG}} \right) - \left(\frac{P_{Mu}}{P_{MM}} \right). \qquad (2)$$

The estimate of SAR used in the present paper is

$$SAR = \sqrt{\frac{P_{GG}}{P_{MM}}} = \sqrt{\frac{P_{G_C} + P_{G_U}}{P_{M_C} + P_{M_U}}} \qquad (3)$$

The true SAR, denoted by a T subscript, is given with the uncorrelated powers set to zero. The estimated SAR is denoted by an Err subscript. If the uncorrelated power on both the microphone and geophone is small compared to the coherent power, equation 3 can be used to approximate the SAR error (E). The error expression is

$$E \equiv \frac{SAR_{Err} - SAR_T}{SAR_T} \approx \frac{1}{2}\left(\frac{P_{G_U}}{P_{GG}}\right) - \frac{1}{2}\left(\frac{P_{M_U}}{P_{MM}}\right). \qquad (4)$$

Equation (4) indicates that the estimated SAR is lowered by uncorrelated power on the microphone and raised by uncorrelated power on the geophone. For the case of no uncorrelated noise on the microphone $E= (1/2)(1-C)$; for the case of no uncorrelated noise on the geophone $E = (-1/2)(1-C)$. Thus $(-1/2)(1-C) \leq E \leq (1/2)(1-C)$. For $C = 0.9$ the error is under 5%; for $C = 0.8$ the error is under 10%. High signal-to-noise (SNR) data produced by a single process commonly have high coherence values.

The coherence of equation (2) is computed with the matlab routine COHERE and the power spectral density (PSD), and cross power spectra of equation (3) are computed with the Matlab routine PSD (Matlab, 1996). For the Aberdeen and Alaska II data, 5 seconds of data blocks were used, a 1.024 s data blocks gives about 1 Hz. resolution. This gives approximately 10 degrees of freedom in the measurement (see Koopmans, 1974, p. 283). For Alaska I data, only 2.048 s recordings were available so we used a 0.48-s data block, with 50% block overlap. This gives roughly eight degrees of freedom. Given the very high signal-to-noise ratios in the data, these processing parameters yield very stable PSD and coherence estimates.

3.0 RESULTS

Data from Alaska II allow direct comparison of SAR as measured from tank noise to SAR measured from a blank pistol shot. The Alaska II data source was a common main battle tank with a piston engine. In those data the vehicle is at distance of 330 m. The microphone PSD, coherence, and SAR are shown in Figure 4. The microphone and geophone have high coherence between 75 and 240 Hz. In this band, the SAR starts near $2.\mathrm{x}10^{-5}$ [(m/s)/Pa] and decreases with frequency. The waveforms, spectra, and SAR from a blank pistol shot fired 1 m above the surface are given in Figure 5. SAR comparisons between the blank pistol shot and the moving tank show excellent agreement.

Figure 4. Results for Alaska II. A) PSD for microphone 16. B) Coherence between microphone 16 and geophone 5 which were separated by 3 m. C) SAR. Vertical lines show frequency alignment for peaks in microphone power with high microphone-geophone coherence and the corresponding SAR. These spectral estimates were formed using 5 s of data broken into blocks of 0.256 s with each block overlapped by 0.52. Squares on the SAR curve (C) indicate the coherence at that frequency bin. The largest to smallest squares have coherence > 0.9, > 0.8, and > 0.7, respectively.

Figure 5. Blank pistol shot results from Alaska II. Microphone number 16 and geophone number 5 are 120 m from the shot. A) Time domain microphone and geophone waveforms. The peak-to-peak amplitudes are 4.0 Pa for the microphone and 3.1×10^{-5} (m/s) for the geophone. B) The PSD energy spectrum for the microphone is in dB relative to 1 Pa^2/Hz, the geophone PSD is relative to 1 $(m/s)^2$/Hz. C) The SAR.
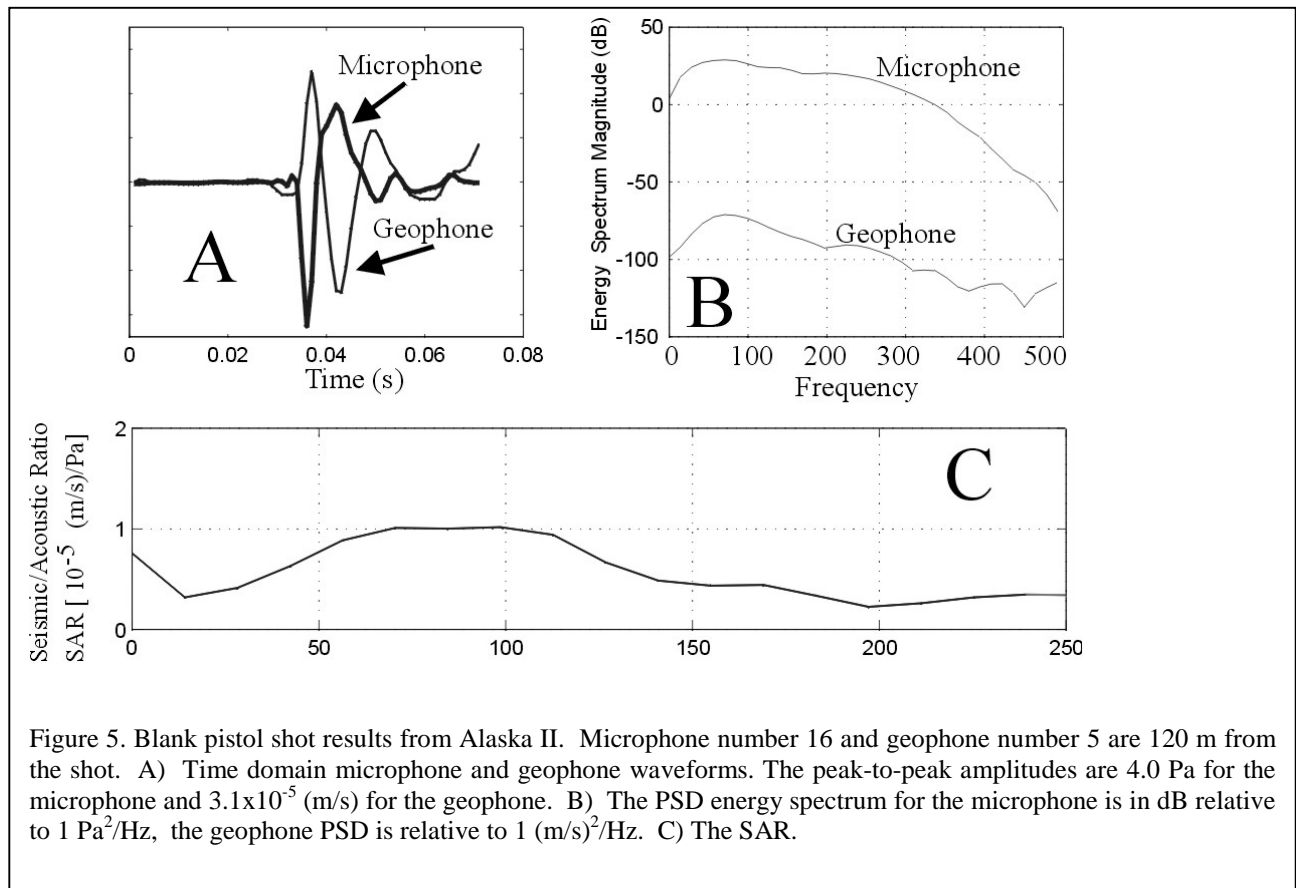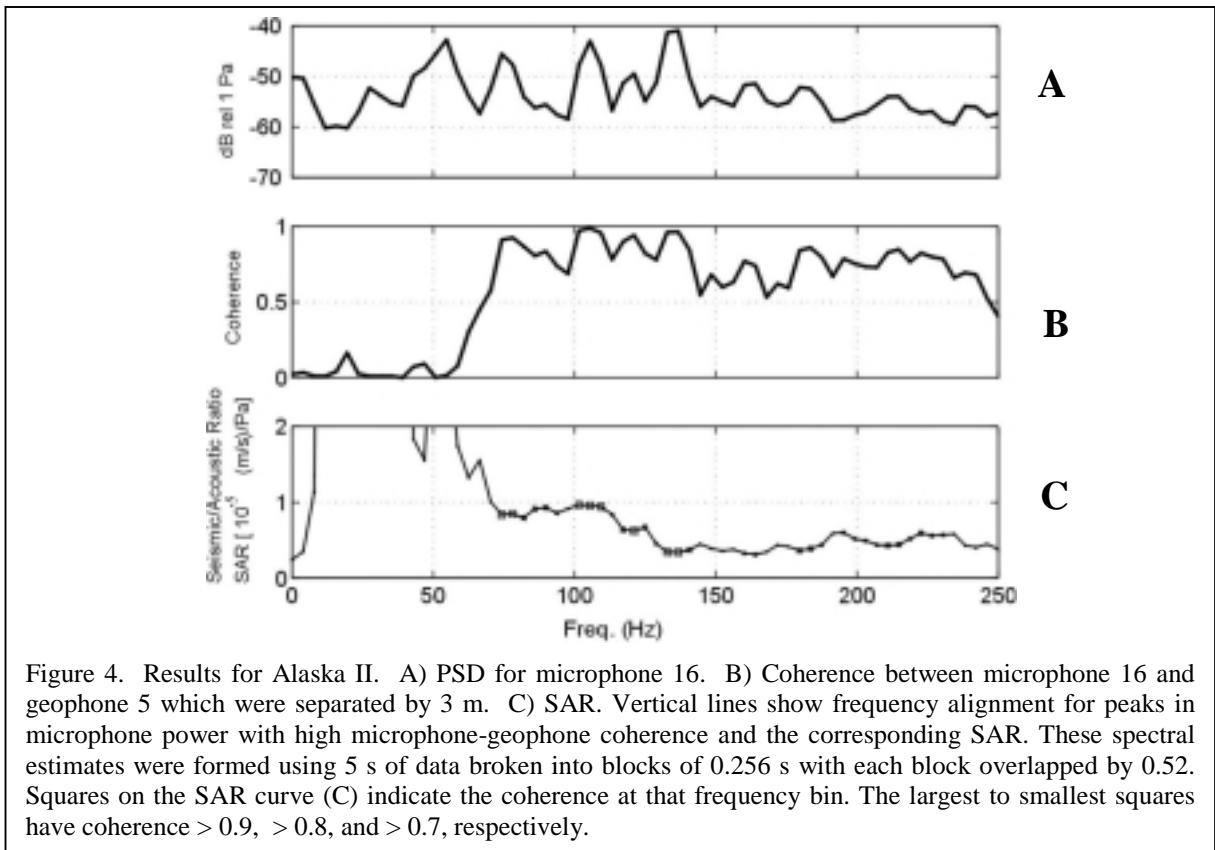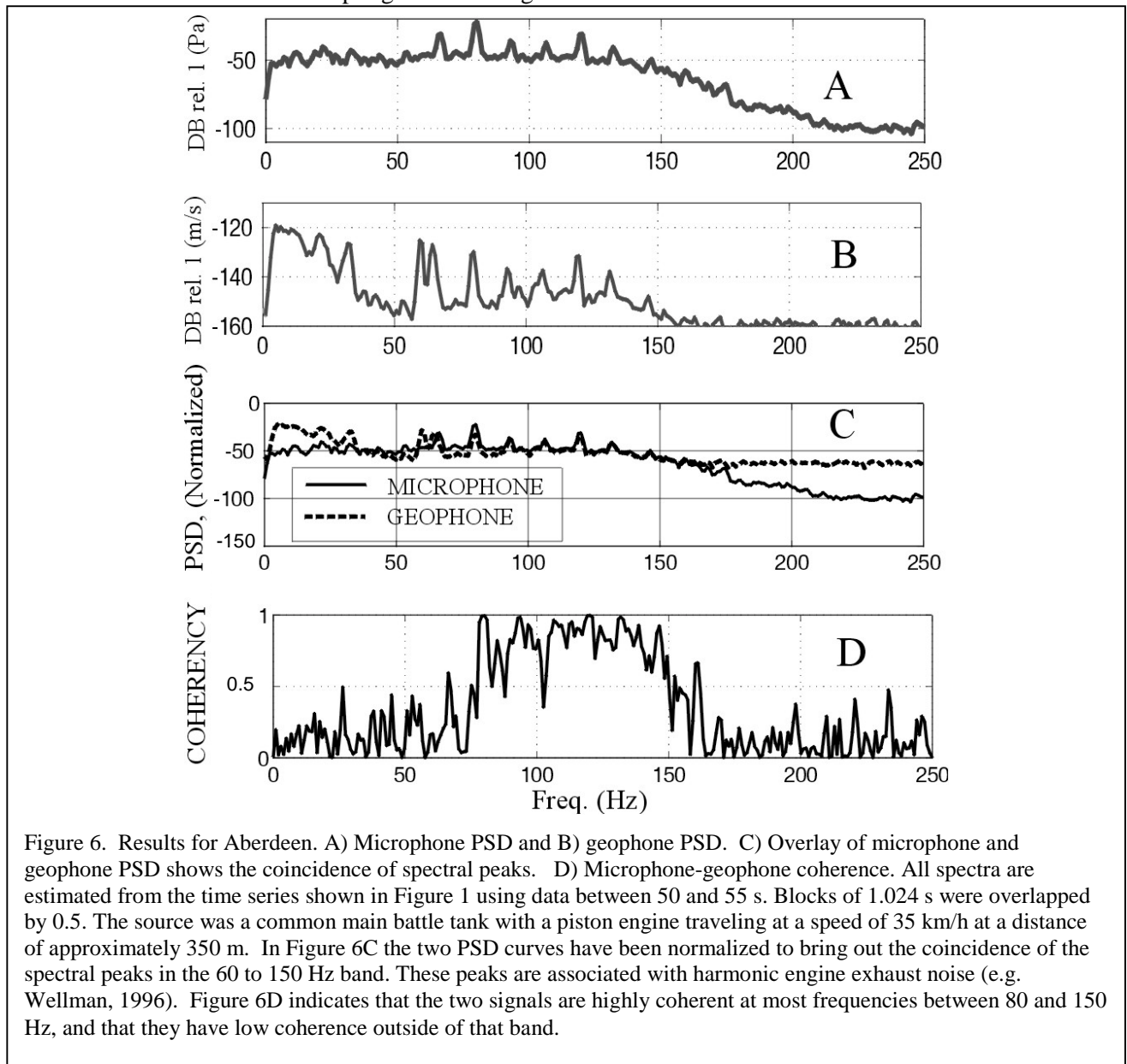
Figure 6 shows microphone and geophone PSD for Aberdeen data. The source was a common main battle tank with a piston engine traveling at a speed of 35 km/h at a distance of approximately 300 m. In Figure 6C the two PSD curves have been normalized to bring out the coincidence of the spectral peaks in the 60-to-150-Hz band. These peaks are associated with harmonic engine exhaust noise (e.g., Wellman, 1996). Figure 6D indicates that the two signals are highly coherent at most frequencies between 80 and 150 Hz, and that they have low coherence outside of that band.

SAR spectra for five Aberdeen data samples are given in Figure 7. The curves in (A), (C), (D), and (E) are produced from the same geophone. All four SAR curves have similar shapes. The scatter is under 3 dB in the 65-to-145-Hz frequency band (coherence > 0.7). For geophone 7 and microphone 8, the SAR has a value of approximately 0.4×10^{-5} [(m/s)/Pa] at 75 Hz rising generally to a value of 1.5×10^{-5} [(m/s)/Pa] at 145 Hz. There is a small local peak at about 105 Hz. The SAR is slightly different for the geophone 9 and microphone 8 pair between 90 and 145 Hz. Geophones 7 and 9 are separated by about 18 m. The SAR peak at about 60 Hz corresponds to electrical pickup on the geophone. It is not a frequency where the seismic to acoustic coupling becomes large.

Figure 6. Results for Aberdeen. A) Microphone PSD and B) geophone PSD. C) Overlay of microphone and geophone PSD shows the coincidence of spectral peaks. D) Microphone-geophone coherence. All spectra are estimated from the time series shown in Figure 1 using data between 50 and 55 s. Blocks of 1.024 s were overlapped by 0.5. The source was a common main battle tank with a piston engine traveling at a speed of 35 km/h at a distance of approximately 350 m. In Figure 6C the two PSD curves have been normalized to bring out the coincidence of the spectral peaks in the 60 to 150 Hz band. These peaks are associated with harmonic engine exhaust noise (e.g. Wellman, 1996). Figure 6D indicates that the two signals are highly coherent at most frequencies between 80 and 150 Hz, and that they have low coherence outside of that band.
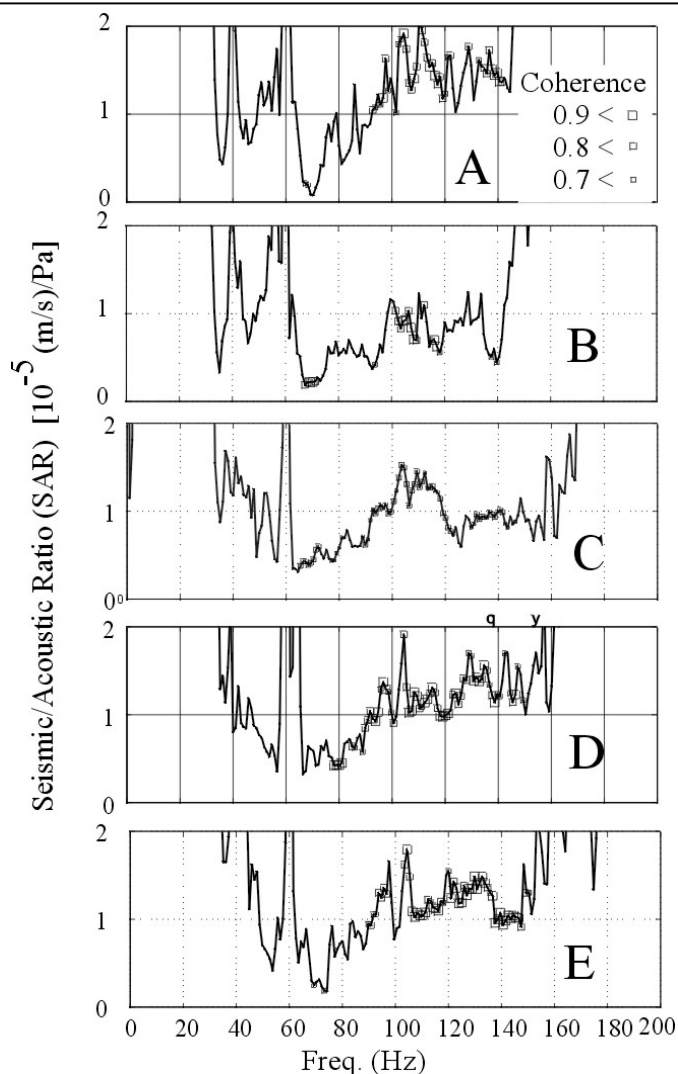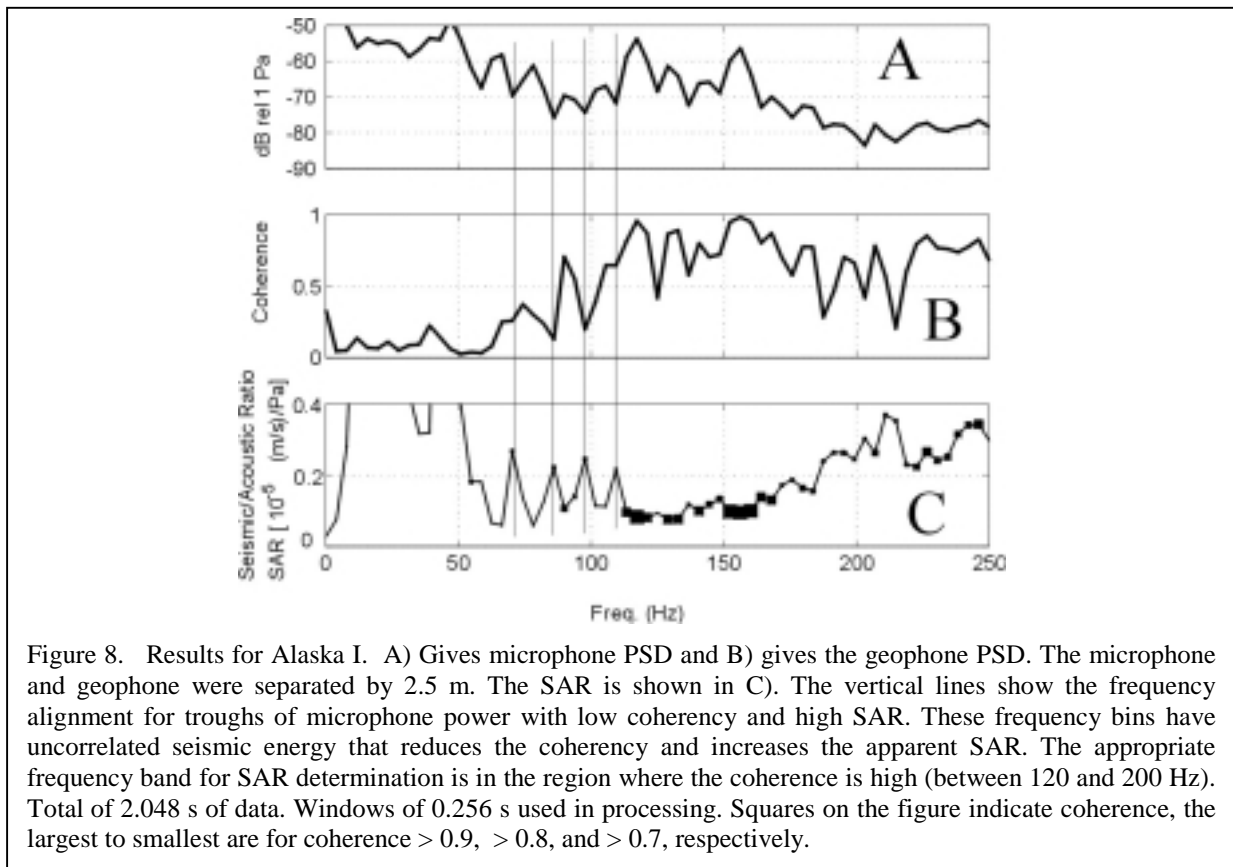
Figure 7. SAR for five data samples from Aberdeen. The source was a common main battle tank with a piston engine traveling at a speed of 35 km/hr. A), C), D), and E) used microphone 8, and geophone 7. These sensors are separated by 9 m. B) used microphone 8 and geophone 9. This pair was also separated by 9 m. The SAR spectra in A), B), C), and D) were estimated at different times during the same vehicle run. The vehicle distance was 600 m in A) and B), 240 m in C), and 270 m in D). The SAR spectrum shown in E) is from a common main battle tank with a turbine engine. In this example, the vehicle was 240 m from the sensors and was traveling at a speed of 25 km/hr. The squares on the SAR curves indicate coherence. The largest to smallest are for coherence > 0.9, > 0.8, and > 0.7, respectively.

The Alaska I data source used the same piston engine battle tank as the Aberdeen data. In this example the vehicle is at distance of 330 m. The microphone PSD, coherence, and SAR are shown in Figure 8. The coherence are generally high from 105 to 200 Hz; however, there are dips in coherence where the microphone PSD is low, and these are indicated by vertical lines on the figure. Where the microphone PSD is high, the coherence is high. At the frequencies where the coherence is relatively low, the SAR is high. This indicates that there is significant seismic energy on the geophone that is not coherent with the microphone signal. In this region it is inappropriate to specify the SAR using equation (3). Conversely, at frequencies where the microphone signal is high the major portion of the geophone power is from acoustic coupling. Thus by following the lower portion of the SAR curve a reliable SAR estimate is obtained. The SAR are around 0.13x10-5   [(m/s)/Pa] at 120 Hz. Rising to about 0.2x10-5 [(m/s)/Pa] at 180 Hz.

In these data sets, our methods for SAR estimation are accurate even for microphone-geophone separations as large as 9 m. This tolerance for large sensor separations is due to the high spatial coherence of the acoustic wave fronts. For example, in the Alaska I data set the average coherence spectra was generally above 0.8 in the 100-to-350-Hz band. In this case average coherence was determined by combining all possible sensor pairs in a large diameter (15 m), 10-element, microphone array. Furthermore, there were high coherence peaks between 50 and 80 Hz. These characteristics are indicative of highly organized acoustic wavefronts.

Figure 8.   Results for Alaska I. A) Gives microphone PSD and B) gives the geophone PSD. The microphone and geophone were separated by 2.5 m. The SAR is shown in C). The vertical lines show the frequency alignment for troughs of microphone power with low coherency and high SAR. These frequency bins have uncorrelated seismic energy that reduces the coherency and increases the apparent SAR. The appropriate frequency band for SAR determination is in the region where the coherence is high (between 120 and 200 Hz). Total of 2.048 s of data. Windows of 0.256 s used in processing. Squares on the figure indicate coherence, the largest to smallest are for coherence > 0.9, > 0.8, and > 0.7, respectively.

4.0 DISCUSSION

The SAR values found at 100 Hz were approximately $1.\times10^{-5}$, 0.1×10^{-5}, and $1.\times10^{-5}$ [(m/s)/Pa] for the Aberdeen, Alaska I, and Alaska II data sets, respectively. The Aberdeen and Alaska II data are consistent with the 0.6×10^{-5} [(m/s)/Pa] (winter) and 0.7×10^{-5} [(m/s)/Pa] (summer) SAR values found by Albert and Orcutt (1989) using blank pistol shots in the time domain. Frequency domain SAR values given by Sabatier et al. (1986a) were centered around 0.3×10^{-5} [(m/s)/Pa] between 100 and 200 Hz are similar to the Alaska I SAR; both of these were considerably lower than Aberdeen or Alaska II. The lower SAR for Alaska I is consistent with high seismic wave velocities observed at that site (P-wave velocity = 4000 m/s; S-wave velocity = 1500 m/s), typical of permafrost. The seismic Rayleigh wave velocities (approximately equal to the S-wave velocity) generated by hammer blows were 180 m/s at Aberdeen, and 150 m/s for Alaska II.

All of the measured SAR values are much lower than values predicted for the simple case of near grazing sound in air on an elastic half space. Using the theory of Ewing, et al. (1957, p. 79) gives the values of SAR shown in Figure 9. A density of 2000 kg/m3 for the ground and 1.2 kg/m3 for air were use in all calculations. When the air wave velocity is near the Rayleigh wave velocity there is a resonant coupling, which greatly increases the SAR. None of the results in these data sets show a sharp spectral peak in the SAR, which would indicate resonant airwave coupling. Thus, it is likely that the high SAR values are due to acoustic to seismic coupling in a shallow air filled poroelastic layer (e.g., Sabatier et al., 1986b). More complex models for the earth, such as incorporating layering and poroelastic material (e.g., Albert, 1993; Attenborough, 1985; Sabatier et al., 1986c), could be used to give a better fit to the observed SAR curve. However, since many of the quantities needed to employ these theories are not presently available for our sites, there is not much to be gained by applying these methods to these data.
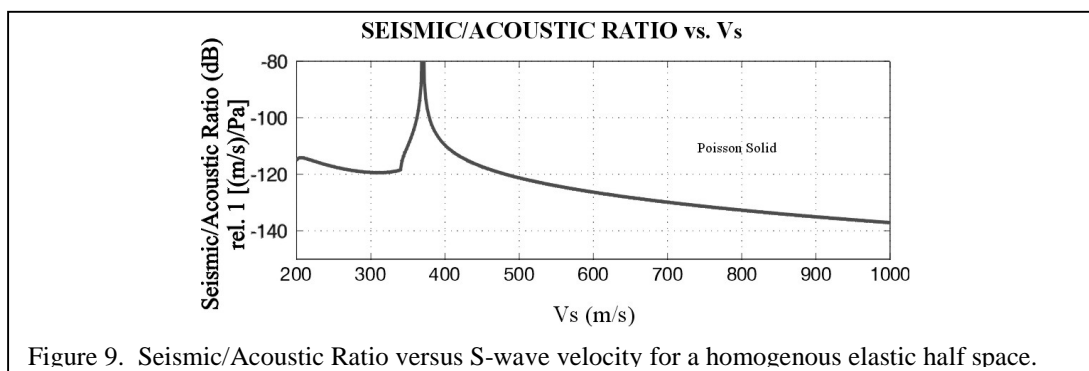

Figure 9. Seismic/Acoustic Ratio versus S-wave velocity for a homogenous elastic half space.

5.0 CONCLUSIONS

Microphone and geophone signals were observed to be highly coherent in frequency bands between 60 to 150 Hz at a grass-covered site, and between 100 to over 200 Hz at frozen snow covered sites. Evidence was presented that support the use of passively recorded signals from moving vehicles to estimate the SAR. This evidence includes the consistency of the SAR values using different vehicle generated noise samples, and comparison of SAR values from vehicle noise with that of a blank pistol shot. The coherence spectrum is used to determine what part of the seismic signal is energy that has propagated as a seismic wave, and what part is due to acoustically induced ground motion. Using the coherence expression we can bound the error in the SAR estimates.

It is possible that prediction error filtering may be useful in removing the acoustic-to-seismic coupled noise on the geophone (Albert, 1984). A through investigation of the SAR values from a variety

of settings may lead to methods for estimating the acoustic ground impedance and the stiffness of the earth's surface. These are important parameters in autonomous remote area monitoring systems.

6.0 ACKNOWLEDGMENTS

7.0 REFERENCES

Albert, D. G., (1984). "The effect of snow on vehicle-generated seismic signatures," CRREL Rpt. 84-23, U. S. Army Corps of Eng., Cold Regions Research and Engineering Laboratory, Hanover, N.H.

Albert, D. G., (1993). "A comparison between wave propagation in water-saturated and air-saturated porous materials." J. Appl. Phys. 73, 28-36.

Albert, D. G., and J. A. Orcutt, (1989). "Observations of low-frequency acoustic-to-seismic coupling in the summer and winter," J. Acoust. Soc. Am. 86, 352-358.

Arcone, S. A., (1998). "Ground-penetrating radar reflection profiling of groundwater and bedrock in an area .of discontinuous permafrost," Geophysics 63(5), 1573-1584.

Attenborough, K. (1985). "Acoustical impedance models for outdoor ground surfaces," J. of Sound and Vib. 9, 521-544.

Ewing, W. M., W. S. Jardetzky, and F. Press, (1957). *Elastic Waves in Layered Media*, (McGraw-Hill New York, NY).

Koopmans, L. H., (1974). *The Spectral Analysis of Time Series*, (Academic, New York, NY).

Matlab, (1996). *Signal Processing Toolbox Users Guide, Version 4*, (The Mathworks, Nadick, MA).

Pewe, T. L., (ed.); (1964). *Guide Book to the Quaternary Geology of Central and South Central Alaska*; Reprinted by the State of Alaska, Department of Natural Resources, Division of Geological and Geophysical Surveys, 50-53.

Sabatier, J. M., H. E. Bass, G. R. Elliott, (1986a). On the location of frequencies of maximum acoustic-to-seismic coupling," J. Acoust. Soc. Am. 80(4), 1200-1202.

Sabatier, J. M., H. E. Bass, L. N. Bolen, K. Attenborough, V.V.S.S. Sastry, (1986c). "The interaction of airborne sound with the porous ground: The theoretical formulation," J. Acoust. Soc. Am. 79, 1345-1352.

Sabatier, J. M., H. E. Bass, L. N. Bolen, and K. Attenborough, (1986b). "Acoustically induced seismic waves," J. Acoust. Soc. Am. 80, 646-649.

Sprague, M. W., R. Raspet, and H. E. Bass, (1993). "Low frequency acoustic ground impedance measurement techniques," Applied Acoustics 39, 307-325.

Wellman, M. (1996). Acoustic feature extraction for target ID," 4th Annual Battlefield Acoustics Symposium, Ft. Meade, MD, 24-26 Sept. 1996.